REPORT DOCUMENTATION PAGE

Form Approved
OMB No. 0704-0188

1. REPORT DATE *(DD-MM-YYYY)*	**2. REPORT TYPE**	**3. DATES COVERED** *(From - To)*
14-06-2006	Technical Paper	

4. TITLE AND SUBTITLE

Quasi-2D Unsteady Flow Solver Module for Rocket Engine and Propulsion System Simulations (Preprint)

5a. CONTRACT NUMBER
FA9300-04-C-0008

5b. GRANT NUMBER

5c. PROGRAM ELEMENT NUMBER

6. AUTHOR(S)
Bryan T. Campbell (Aerojet); Roger L. Davis (UC Davis)

5d. PROJECT NUMBER
502603BQ

5e. TASK NUMBER

5f. WORK UNIT NUMBER

7. PERFORMING ORGANIZATION NAME(S) AND ADDRESS(ES)

Aerojet
P.O. Box 13222
Sacramento CA 95813-6000

8. PERFORMING ORGANIZATION REPORT NUMBER

AFRL-PR-ED-TP-2006-189

9. SPONSORING / MONITORING AGENCY NAME(S) AND ADDRESS(ES)

Air Force Research Laboratory (AFMC)
AFRL/PRS
5 Pollux Drive
Edwards AFB CA 93524-7048

10. SPONSOR/MONITOR'S ACRONYM(S)

11. SPONSOR/MONITOR'S NUMBER(S)
AFRL-PR-ED-TP-2006-189

12. DISTRIBUTION / AVAILABILITY STATEMENT

Approved for public release; distribution unlimited (AFRL-ERS-PAS-2006-137)

13. SUPPLEMENTARY NOTES
Presented at the 42nd AIAA/ASME/SAE/ASEE Joint Propulsion Conference, Sacramento, CA, 9-12 July 2006.

14. ABSTRACT

A new quasi-two-dimensional procedure is presented for the transient solution of real-fluid flows in lines and volumes including heat transfer effects. The solver is targeted to the commercial dynamic simulation software package Simulink® for integration into a larger suite of modules developed for simulating rocket engines and propulsion systems. A Fortran95 code using more conventional solution procedures is being developed in parallel to provide verification test cases. The solution procedure for both codes is coupled with a state-of-the-art real-fluids property database so that both compressible and incompressible fluids may be considered using the same procedure. The numerical techniques used in this procedure are described. Test cases modeling transient flow of nitrogen, water, and hydrogen are presented to demonstrate the capability of the current technique.

15. SUBJECT TERMS

16. SECURITY CLASSIFICATION OF:			**17. LIMITATION OF ABSTRACT**	**18. NUMBER OF PAGES**	**19a. NAME OF RESPONSIBLE PERSON**
					Mr. Sean Kenny
a. REPORT	**b. ABSTRACT**	**c. THIS PAGE**	A	12	**19b. TELEPHONE NUMBER** *(include area code)*
Unclassified	**Unclassified**	**Unclassified**			N/A

Quasi-2D Unsteady Flow Solver Module for Rocket Engine and Propulsion System Simulations (Preprint)

Bryan T. Campbell*
Aerojet, Sacramento, CA, 95813-6000

and

Roger L. Davis†
University of California, Davis, Davis, CA, 95616

A new quasi-two-dimensional procedure is presented for the transient solution of real-fluid flows in lines and volumes including heat transfer effects. The solver is targeted to the commercial dynamic simulation software package Simulink® for integration into a larger suite of modules developed for simulating rocket engines and propulsion systems. A Fortran95 code using more conventional solution procedures is being developed in parallel to provide verification test cases. The solution procedure for both codes is coupled with a state-of-the-art real-fluids property database so that both compressible and incompressible fluids may be considered using the same procedure. The numerical techniques used in this procedure are described. Test cases modeling transient flow of nitrogen, water, and hydrogen are presented to demonstrate the capability of the current technique.

Nomenclature

A	=	cross-sectional area
A_p	=	perimeter
a_r	=	relative acceleration between inertial and absolute frames of reference
c	=	fluid speed of sound
c_w	=	wall material specific heat
D	=	flow passage hydraulic diameter
E	=	fluid total energy = $\rho\,(e + u^2/2 + gz)$
e	=	fluid internal energy
f	=	fluid friction coefficient
F	=	vector of fluid mass, momentum, and energy fluxes
g	=	gravitational acceleration
h	=	forced convection heat transfer coefficient
H	=	fluid static enthalpy referenced to fluid normal boiling point at 1atm
i	=	cell index
K	=	minor loss coefficient
k	=	fluid thermal conductivity
k_w	=	wall material thermal conductivity
L	=	domain length
Nu_D	=	Nusselt number based on hydraulic diameter ($Nu_D = hD/k$)
p	=	fluid static pressure
Pr_f	=	fluid Prandtl number evaluated at film temperature ($Pr = c_p \mu / k$)
q_w	=	heat flux from wall to fluid
Re_D	=	local flow Reynolds number based on hydraulic diameter ($Re_D = \rho u D/\mu$)
Re_f	=	local flow Reynolds number based on hydraulic diameter evaluated at film temperature

* Engineering Specialist, Systems Engineering, P.O. Box 13222, Dept. 5271, AIAA Member.
† Professor, Mechanical and Aeronautical Engineering, AIAA Associate Fellow.

S = source vector
t = time
T_B = fluid bulk temperature
T_f = film temperature ($T_f = (T_w+T_B)/2$)
T_w = wall temperature
U = fluid state vector
u = fluid absolute velocity
u_r = relative velocity of moving frame of reference
V = fluid cell volume
x = distance along solution domain
z = elevation above reference plane
Δx_i = length of computational cell i
ε = wall roughness height
ρ = fluid density
ρ_w = wall material density
τ_w = shear force between wall and fluid (friction)
μ = fluid molecular viscosity

I. Introduction

THIS paper addresses development of a quasi-two dimensional (2D), unsteady, two-phase flow solver with real-fluid properties suitable for use in system-level transient simulations of hydraulic and pneumatic systems and, in particular, rocket engine and propulsion systems. The flow solver module described here is an integral part of a rocket engine system modeling tool currently under development. The solver is geared towards modeling the dynamic behavior of fluid-filled lines and passages (i.e., the solution domain is much larger in one dimension than in the others) where heat transfer and phase change are important. Existing software models available for such simulations are typically based on lumped analysis approaches, which do not fully capture the flow dynamics, mainly due to the elimination of the unsteady momentum terms. Although so-called "continuity" waves can be captured using a lumped analysis, neglecting these terms leads to an inability to capture true "dynamic" waves required for simulating such phenomenon as water-hammer and pressure surge[1]. Since these phenomena play an important role in the operation and testing of liquid rocket engines and propulsion systems, a method that captures these effects is desired.

Several approaches for simulating the dynamic behavior of such "fluid-transmission" lines have been reported. The "lumped-analysis" approach treats a flow passage as a series of fluid control volumes that conserve mass and energy linked by flow resistance elements that compute the flow between the volumes[2]. While this approach does conserve momentum in a quasi-steady sense at the flow resistances, the unsteady momentum term in the governing equations is neglected. Another approach uses the Method of Characteristics[3], which is a general method for solving hyperbolic partial differential equations. The governing equations for fluid flow are compatible with this method and it has been used for simulation of fluid transmission lines[4]. While the unsteady momentum terms are retained using this method, other problems, particularly at the boundaries of components, make it problematic to apply to a modular system-level simulation tool. Modal methods have also been used when solution in the frequency domain is possible[5]. This technique represents the pressure and flow distribution in the flow domain as a sum of an infinite series of mode shapes, similar to a Fourier series solution. While this method presents an elegant and efficient method for simulating simple flow situations (e.g., incompressible flow, inviscid flow, laminar flow, etc.), the addition of turbulent flow, real-fluid properties, heat transfer, and phase change complicate application of the method and reduce its attractiveness.

The current technique focuses on application of standard finite-volume methods to the development of an unsteady flow solver capable of capturing wave dynamics, real-fluid effects, heat transfer, and phase change. In addition, the solution method must be computationally efficient enough to operate as a module in a larger system-level simulation. The following sections describe the modeling approach, numerical methodologies, and test cases that have been used during development of this model.

II. Approach

The intention of the model developed here is to represent fluid lines and flow passages as a quasi-2D domain. The intended components to be modeled using this method are fluid lines and internal flow passages where the length of the domain is much larger than the hydraulic diameter of the domain. Flow separations and non-axial

velocities are minimal for these types of components; hence, the quasi-2D assumption is valid. The solver is targeted to the commercial Simulink® dynamic simulation software package from The MathWorks for integration into a larger suite of modules developed for simulating rocket engines and propulsion systems. Simulink® was selected since it offers a wide range of capabilities, over a dozen robust differential equation solvers, extensive documentation and technical support, a modern graphically based modeling paradigm, an existing user community across many disciplines, and commercially funded code development and maintenance. A Fortran95 code is also being developed in parallel[6] to provide test cases for the Simulink® module.

The solver is being developed to model the effects of variable area along the length of the domain, friction, minor losses (e.g., bends), real-fluid and two-phase flow effects, gravity and acceleration effects, heat transfer, and the capability to produce unsteady and steady-state solutions. Fluid equation of state closure is provided by the REFPROP fluid property database[7] available from the National Institute for Standards and Testing (NIST). This database uses state-of-the-art Equation of State models to fully describe "real-fluid" properties over a wide range of thermodynamic conditions, including liquid, vapor, mixed phase, and supercritical fluid regimes. Properties that completely define the fluid thermodynamic state, as well as transport properties, are available as a function of any two thermodynamic parameters. Validated fluid models for over 80 pure fluids and over 180 fluid mixtures are available in the database. The database is accessed through a suite of Fortran subroutines that were compiled into the codes and obtain fluid equation of state model parameters from external files.

Friction and heat transfer are modeled as source terms in the fluid governing equations. This approach allows the flow to be modeled as one-dimensional (1D) and facilitates computational efficiency. Friction (i.e., viscous losses and losses due to bends and fittings) and heat transfer coefficients are obtained from suitable correlations between the flow variables and source terms.

III. Governing Equations

The modeling procedure solves differential equations representing the physics of the problem. Equations are presented below for modeling the fluid dynamics, wall temperature, and source terms coupling the two.

A. Fluid

The differential equations governing the dynamics of the fluid consist of the quasi two-dimensional continuity, Navier-Stokes and energy equations simplified to model viscous effects and general acceleration in a non-inertial frame using source terms[8].

$$\frac{1}{V}\frac{\partial UV}{\partial t}+\frac{\partial F}{\partial x}=\frac{S}{V} \tag{1}$$

$$U=\begin{vmatrix}\rho\\ \rho u\\ E\end{vmatrix},\quad F=\begin{vmatrix}\rho u_r\\ (\rho u u_r+p)\\ \rho u_r H\end{vmatrix},\quad S=\begin{vmatrix}0\\ \frac{pV}{A}\frac{dA}{dx}-\rho V a_r-\tau_w dx A_p-K\frac{\rho u_r^2}{2}A\\ \frac{\dot{q}_w}{V}-\tau_w u_r dx A_p-K\frac{\rho u_r^3}{2}A\end{vmatrix} \tag{2}$$

B. Wall

The wall bounding the fluid computational domain is modeled using standard control volume methods for heat transfer[9]. Forced convection heat transfer between the fluid and wall as well as heat conduction within the wall are included in the model. Heat conduction between the wall and fluid is neglected due to its small magnitude compared to forced convection heat transfer. In addition, conduction in the wall is modeled as 1-D neglecting radial conduction. These effects can be added to the model as required.

Based on these assumptions, the governing equation for heat transfer within the wall is[9]:

$$\frac{\partial T_w}{\partial t}=\frac{1}{\rho_w c_w}\frac{\partial}{\partial x}\left(k_w\frac{\partial T_w}{\partial x}\right) \tag{3}$$

Eq. (3) does not include the contribution due to forced convection heat transfer between the fluid and the wall. It is more convenient to add this term below to the discretized equations.

C. Source Terms

Equations (1) through (3) above require several source terms that are a function of the wall and fluid conditions. The wall shear stress can be related to a suitable friction factor, *f*, which is a function of the local Reynolds number and wall surface roughness. For single-phase flow in pipes, the Churchill correlation[10] can be used to determine wall friction factors using the equation:

$$f = \frac{\tau_w}{\rho u_r^2} = \left[\left(\frac{8}{Re_D} \right)^{12} + \frac{1}{(A+B)^{3/2}} \right]^{1/12}, \; A = \left[2.457 \cdot ln\left(\frac{1}{(7/Re_D)^{0.9} + 0.27(\varepsilon/D)} \right) \right]^{16}, \; B = \left(\frac{37{,}530}{Re_D} \right)^{16} \tag{4}$$

Similarly, forced convection heat transfer between the wall and fluid can be obtained using a suitable correlation. For single-phase flow in pipes, the Colburn correlation[11] can be used to determine the forced convection heat transfer from the wall to fluid:

$$\dot{q}_w = h \cdot A_p \cdot (T_w - T_B), \; Nu_D = \frac{hD}{k} = 0.023 \cdot Re_f^{0.8} \cdot Pr_f^{1/3} \tag{5}$$

The source term correlations given here are suitable for single-phase flows of non-specific fluids. Other fluid-specific and/or two-phase correlations can be substituted to model other types of flows as required.

D. Boundary Conditions

Boundary conditions are applied each time-step at the inlet and exit of each line in a network. These boundary conditions are specified depending on network connectivity and consist of a global inlet, global exit, or junction boundary condition. At the global inlet(s) to the network, the stagnation enthalpy and entropy are specified based on a given stagnation pressure and stagnation temperature and the predicted velocity. Resulting fluid density and internal energy are determined from REFPROP, thus allowing for determination of the fluid states at the inlet. At the global exit(s) to the network, the static pressure is specified. The internal energy and velocity states along with this specified pressure are used with REFPROP to determine density and total energy. The prescribed inlet and exit conditions may be specified as functions of time. At line junctions, the contributions of the time-rate changes in the primary variables contained in U of Eq. (1) and T_w of Eq. (3) are summed to give total time-rate change at the junction node. For each junction of a given line, the neighboring line numbers and boundaries (i.e., inlet or exit) are stored to make implementation of this boundary condition straightforward.

IV. Numerical Methods

Equations (1) through (3) may be solved with a variety of numerical schemes that are second-order accurate in space and time for "steady" or transient flow. The flow solver is implemented using an ANSI C S-Function, which is a specialized program for use in Simulink® models that contains specific subroutines required during model execution. The model states are the flow and wall variables contained in the U vector and T_w at each computational node and the main subroutine of the S-Function computes the time derivatives of the flow states (dU/dt and dT_w/dt). Once time derivatives of the system states are computed, standard Simulink® solvers are used to integrate the derivatives and compute the time history of the model states. Multiple numerical schemes have been implemented in the Fortran95 code to provide flexibility and robustness when solving for different flow conditions. This version of the code uses solution methods similar to those discussed here and is described in more detail elsewhere[6].

A. Computational Grid

The governing differential equations are solved on a 1-D grid with varying area as shown in Fig. 1. In general, the computational domain has N computational cells. The fluid states (U) are located at the cell faces, as shown in the figure. The wall states (T_w) are located in the wall at the midpoint of the cells as shown. This staggered arrangement was selected to simplify application of boundary conditions for the fluid and wall. Thus, for N cells, there are $3(N+1)$ fluid states and N wall states.

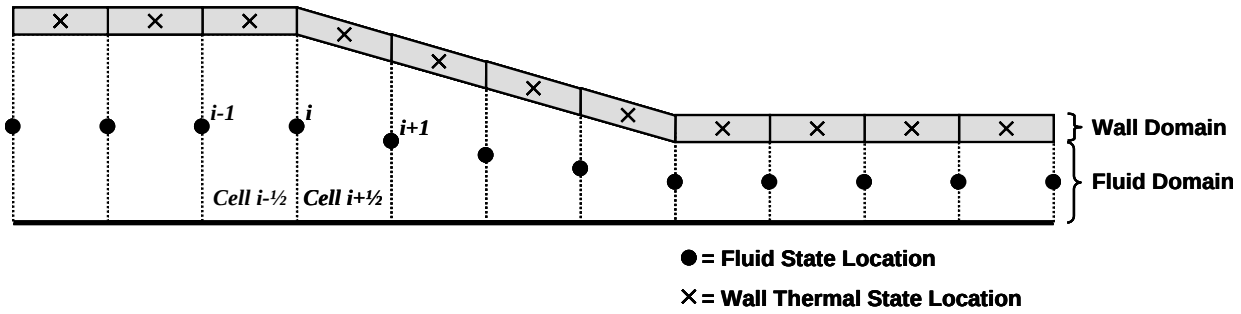

Figure 1. Computational grid.

B. Discretization

As discussed above, the main subroutine of the flow solver S-Function computes the model state derivatives (dU/dt and dT_w/dt) at each computational node. A finite-volume method is used to compute the fluid-state fluxes at the center of each fluid cell, so for cell $i+½$ in Fig. 1:

$$\left(\frac{\Delta U}{\Delta t}\right)_{i+1/2} = S_{i+1/2} - \left(\frac{F_{i+1}\cdot A_{i+1} - F_i \cdot A_i}{V_{i+1/2}}\right) \tag{6}$$

The fluid-state fluxes from each cell are distributed to the fluid-state derivatives computed at the neighboring faces:

$$\left(\frac{dU}{dt}\right)_i = 0.5\cdot\left[\left(\frac{\Delta U}{\Delta t}\right)_{i-1/2} + \left(\frac{\Delta U}{\Delta t}\right)_{i+1/2}\right] \tag{7}$$

A similar method is used to compute wall-state fluxes at the center of each wall cell[9]; however, since the wall states are at the center of the wall cells—no distribution of fluxes is required:

$$\left(\frac{dT_w}{dt}\right)_i = \left(\frac{1}{\rho_w \cdot c_{w_i}\cdot \Delta x_i}\right)\left[\frac{k_+\left(T_{w_{i+1}} - T_{w_i}\right)}{x_{i+1}-x_i} - \frac{k_-\left(T_{w_i} - T_{w_{i-1}}\right)}{x_i - x_{i-1}} - \dot{q}_{w_i}\right] \tag{9}$$

where the wall material specific heat (c_w) is a function of local wall temperature, and k_+ and k_- are weighted wall thermal conductivity values for neighboring cells computed using the harmonic mean discussed in Reference 9. Note that the forced convection heat transfer between the wall and fluid has been introduced.

C. Temporal Solution

Once the state derivatives are computed at each computational node, standard Simulink® solvers are used to solve the discretized equations as a function of time. Four variable-step solvers were investigated for solving Eqs. (1) through (3) on the computational domain, all of which are suited to stiff systems of differential equations like those considered here. The most rigorous of these is the implicit solver ode23s, which is a one-step solver based on a modified Rosenbrock formula of order two[12]. Ode15s is a multi-step solver based on Numerical Differentiation Formulas (NDFs)[12], which are related to the backward differentiation formulas (also known as Gear's method) but are more efficient[13]. Ode23t is an implementation of the trapezoidal rule using a "free" interpolant that is effective for moderately stiff problems[13]. Ode23tb uses the TR-BDF2[14] two-stage procedure where the first stage is a trapezoidal rule step and the second stage is a backward differentiation formula of order two[13]. References 12 and 13 provide additional details.

V. Results

Several test cases have been generated to evaluate the merits of the procedure described here. Solutions were obtained with both the Simulink® code and Fortran95 version of the solver. Results are presented below.

A. Compressible Flow in a Pipe

A transient pipe flow simulation of gaseous nitrogen in a pipe has been performed to demonstrate the capability of the present procedure for compressible flows. A 0.254 m (10 in.) pipe with a 0.0254 m (1 in.) diameter and 90-deg elbow at 0.127 m (5 in.) was used for these simulations as shown in Fig. 2. The surface roughness of the pipe was 2.54×10^{-6} m (0.0001 in.), a typical value for commercially smooth pipe. The inlet total as well as initial exit static pressure were held at 345 kPa (50 psia). The inlet total temperature was held at 300°K (540°R). Thus, the initial velocity of flow in the pipe was zero. At 0.001 seconds, the exit static pressure was reduced to 331 kPa (48 psia) over 0.001 seconds (linear ramp). This reduction in pressure simulates a fast-acting valve opening downstream of the line, which initiates a series of expansion and compression waves in the pipe and an increase in flow velocity. At steady-state, static pressure in the pipe settles to a non-uniform distribution along the length of the pipe with inlet pressure higher than exit due to friction losses. The flow velocity grows asymptotically until it reaches a steady-state distribution. The simulation was run to steady-state when both pressure and velocity distributions remain time-independent. A total of 32 cells with uniform spacing were used along the pipe to discretize the governing equations.

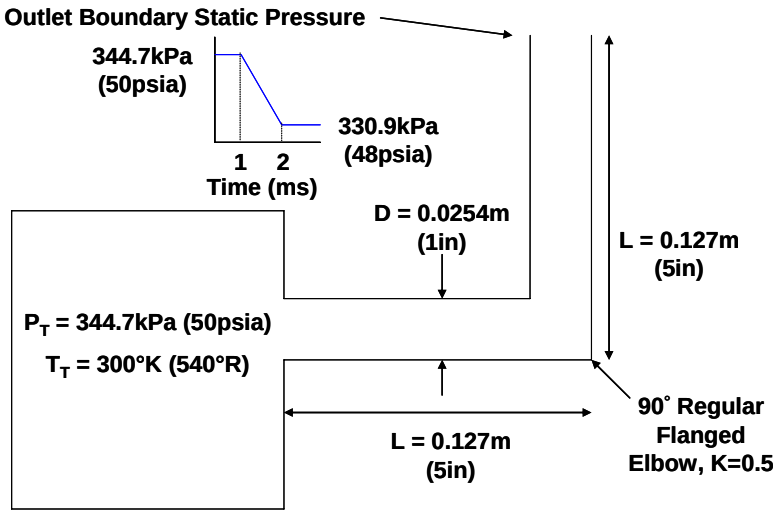

Figure 2. Simple pipe geometry.

Figure 3 shows the predicted pressure, velocity, and enthalpy as a function of time using the implicit Simulink® solver ode23s. Sinusoidal variation of pressure with time is evidence of the expansion and compression waves propagating through the pipe. Time-variation of the velocity corresponds to these waves. Velocity increases until it reaches an average value of 65.9 m/s (216.3 ft/s). Figure 4 shows the pressure, velocity, and enthalpy distributions at steady-state. Pressure and enthalpy decrease along the length of the pipe due to viscous effects, with a large jump at 0.127 m (5 in.) due to the minor loss in the elbow. Figure 5(a) compares transient pressure predictions of the model at the mid-point of the pipe using four different Simulink® solvers. The solvers, based on the NDF equations (ode15s), trapezoidal rule (ode23t), and TR-BDF2 solver (ode23tb), give very similar results to the implicit solver (ode23s). However, these solvers run in about 4 percent of the computational time required for the implicit solver (7,443 seconds for the 0.02 second simulation), making them attractive for quick turn-around analyses. The NDF solver only slightly under-predicts the pressure oscillation frequency after three cycles while the other solvers show better agreement to frequency and amplitude of the implicit solver results. Finally, Fig. 5(b) compares the pressure solution obtained with the implicit solver (ode23s) with the solution obtained using the explicit version of the Fortran code discussed in Reference 6. The two solvers produce very similar results with only small differences between pressure wave amplitude and frequency. The 0.02 second Fortran simulation runs in about 135 seconds using the explicit solver, or in about half the time of the faster Simulink solvers. This comparison gives an estimate of the computational overhead associated with using Simulink for this type of calculation.

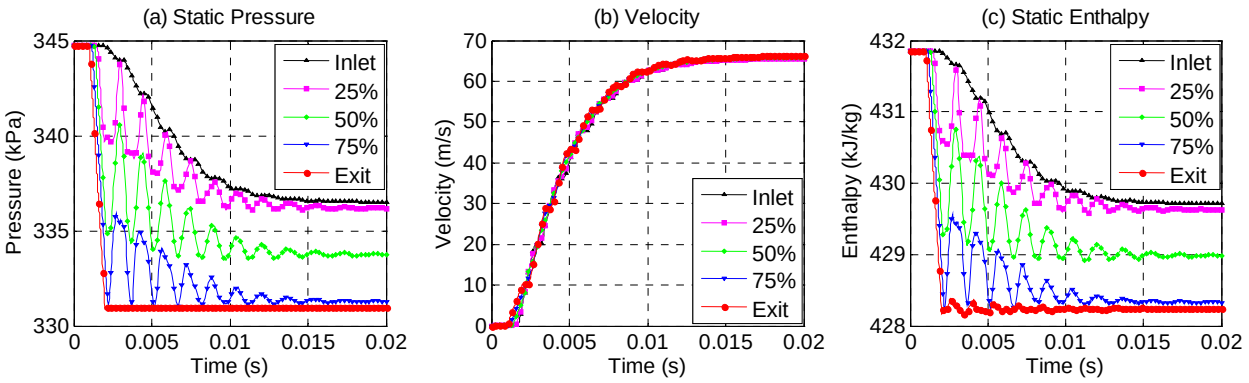

Figure 3. Nitrogen transient pipe flow.

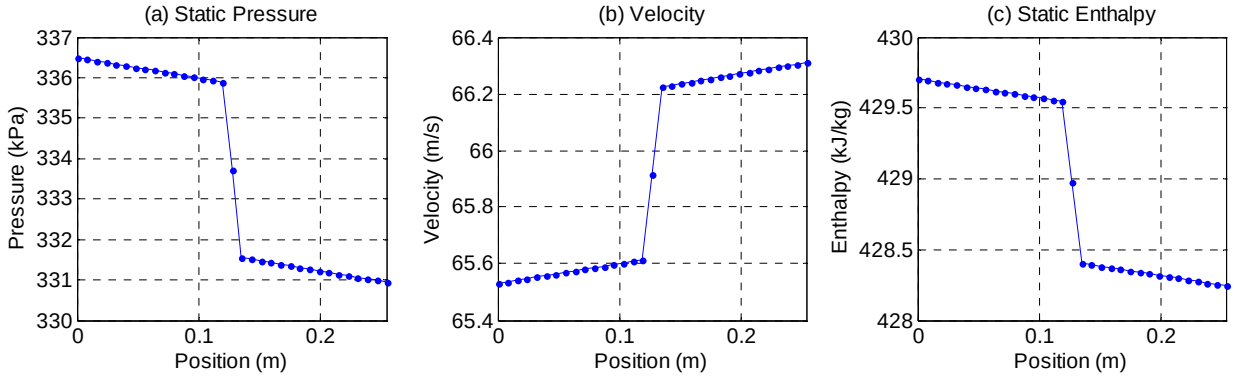

Figure 4. Nitrogen pipe flow at steady-state.

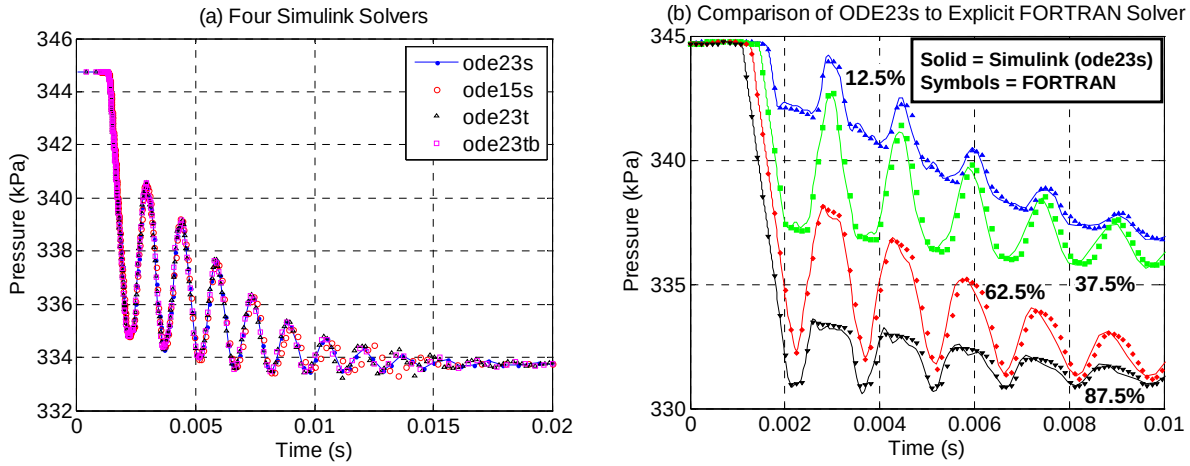

Figure 5. Transient solution with various solvers.

A hand calculation[6] for the steady-state case assuming incompressible flow yields a static pressure drop of 5.4095 kPa (0.7846 psid) and flowrate of 0.1275 kg/s (0.2810 lbm/s). The simulation yields a steady-state static pressure drop of 5.5480 kPa (0.8047 psid) and flowrate of 0.1264 kg/s (0.2788 lbm/s). Thus, the simulation results differ from the hand calculations by 2.6 percent in pressure and 0.8 percent in flow. However, the hand calculation is expected to have some error due to the incompressibility assumption. Thus, the steady-state simulation results are verified by independent hand calculations.

The period of pressure oscillations can be compared to the period expected for frictionless flow (e.g., organ pipe modes) as a check of the transient response of the computational solution. The pressure waves inside the pipe travel at slightly less than the speed of sound, where the difference is a result of friction losses. Thus, pressure oscillations should occur close to the natural frequency of the pipe (c/2L), or 696Hz for this case. The oscillation period of the

first wave in the simulation is 0.00147 seconds, which is slightly higher than the period corresponding to the natural frequency of the pipe (0.00144 seconds). The period of subsequent waves is longer due to the increasing effects of friction losses as flow velocity increases. Thus, the method produces transient results in keeping with physical expectations.

B. Incompressible Flow in a Pipe

The same configuration described above in Fig. 2 was used for water flow simulation to demonstrate the capability to predict transient flows in essentially incompressible fluids. The critical difference for incompressible fluids is that wave speeds are much larger than in compressible fluids, resulting in smaller time steps for numerical stability. The same time-dependent boundary conditions as discussed above are imposed on the inlet and outlet planes of the pipe. Figures 6 and 7 show the transient and steady-state solutions for the water flow simulation computed using solver ode23tb (the TR-BDF2 solver) with a maximum time step of 1×10^{-5} seconds. Small amplitude pressure oscillations are evident throughout the duration of the simulation, and the flow relaxes gradually to its equilibrium state. The time to reach steady-state for water is much longer than that required for nitrogen due to the incompressibility of the fluid. At steady-state, the flow velocity is nearly constant, as expected for a nearly incompressible fluid. Figure 8 shows the first 0.004 seconds of static pressure and enthalpy variation (velocity variation is initially negligible) and demonstrates good agreement of the Simulink results to the explicit version of the Fortran code for oscillation frequency and magnitude.

As with the nitrogen case, the steady-state water solution can be compared to a hand calculation for the same conditions. Both the hand calculation and simulation yield flowrates of 2.0508 kg/s (4.5213 lbm/s) and static pressure drops of 5.5762 kPa (0.8088 psid). The agreement between the hand calculation and simulation is better for water since the assumption of incompressible flow is more correct for water compared to gaseous nitrogen.

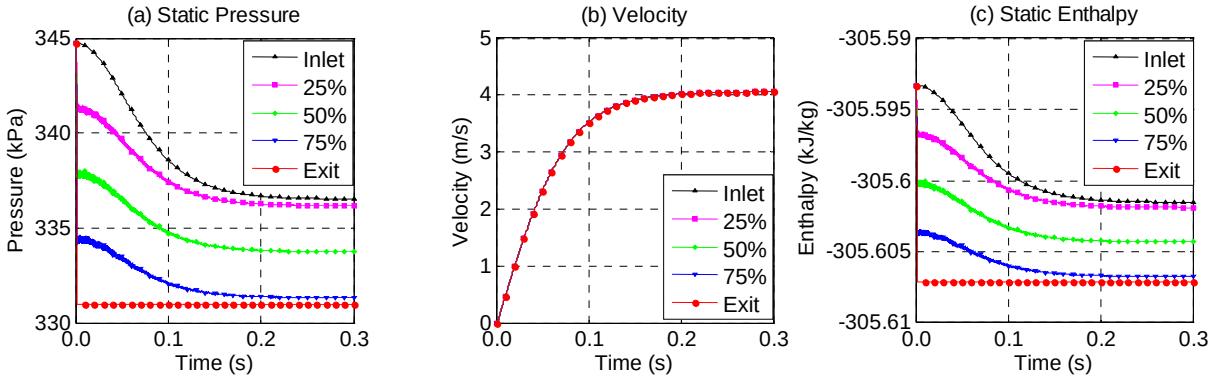

Figure 6. Water transient pipe flow.

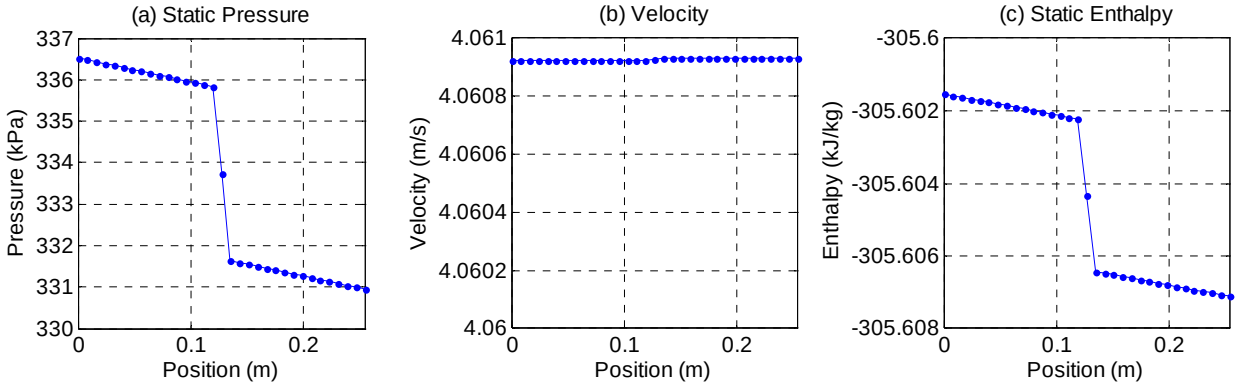

Figure 7. Water pipe flow at steady-state.

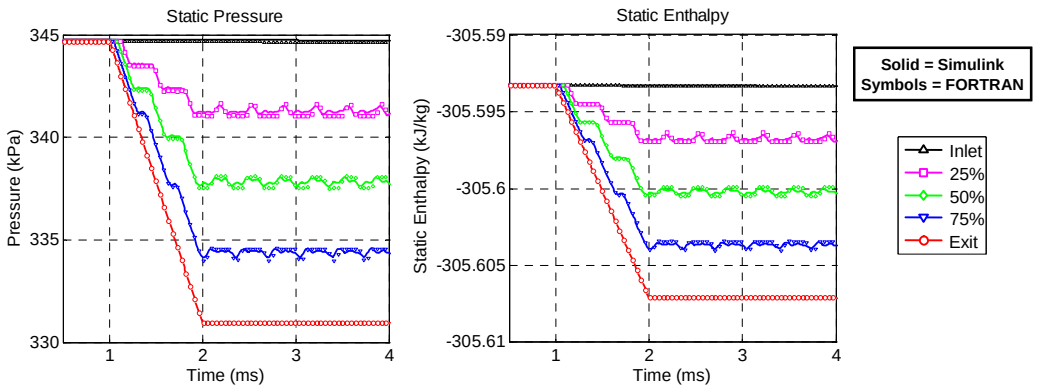

Figure 8. Comparison of water transient results with Fortran code.

C. Cryogenic Fluids With Heat Transfer

The current procedure can also be used to solve for transient behavior of cryogenic fluids, including heat transfer between fluid and pipe. A simple case similar to the one described above was modeled with liquid parahydrogen to demonstrate this capability. A 0.6096 m (24 in.) long straight pipe with an inner diameter of 0.0254 m (1 in.) and surface roughness of 2.54×10^{-6} m (0.0001 in.) was used. The initial fluid temperature was set at 22.22 °K (40° R) and initial pressure was 345 kPa (50 psia). Inlet total pressure was held at 345 kPa (50 psia) and inlet total temperature was held at 22.22 °K (40 °R). Thus, the initial flow velocity in the pipe was zero. The copper pipe had a 0.003175 m (0.125 in.) thick wall, which was initially set to the same temperature as the fluid. At 0.001 seconds, the exit static pressure was reduced to 331 kPa (48 psia) over 0.001 seconds (linear ramp). The pipe wall was subjected to zero heat transfer at the inlet and outlet boundaries. The conditions for this problem were chosen to avoid two-phase flow since this capability is currently not implemented. The problem was modeled using the TR-BDF2 solver (ode23tb) with a maximum time step of 1×10^{-5} seconds and 32 computational cells along the domain. While temperature change of the wall is expected to be small for this case, it demonstrates the capability to model conjugate heat transfer using this procedure.

Figures 9 and 10 show the transient and steady-state fluid solutions for the liquid hydrogen flow simulation. Pressure oscillations of moderate amplitude are evident throughout the duration of the simulation, and the flow relaxes gradually to its equilibrium state. Since liquid hydrogen compressibility is lower than gaseous nitrogen and higher than liquid water, its behavior is between the previous cases. The time to reach steady-state is similar to the water case. At steady-state, the flow velocity is nearly constant, as expected for a fluid with low compressibility. Figure 11 shows the first 0.006 seconds of static pressure and enthalpy variation (velocity variation is initially negligible) and demonstrates good agreement of the Simulink results to the explicit version of the Fortran code for oscillation frequency and magnitude.

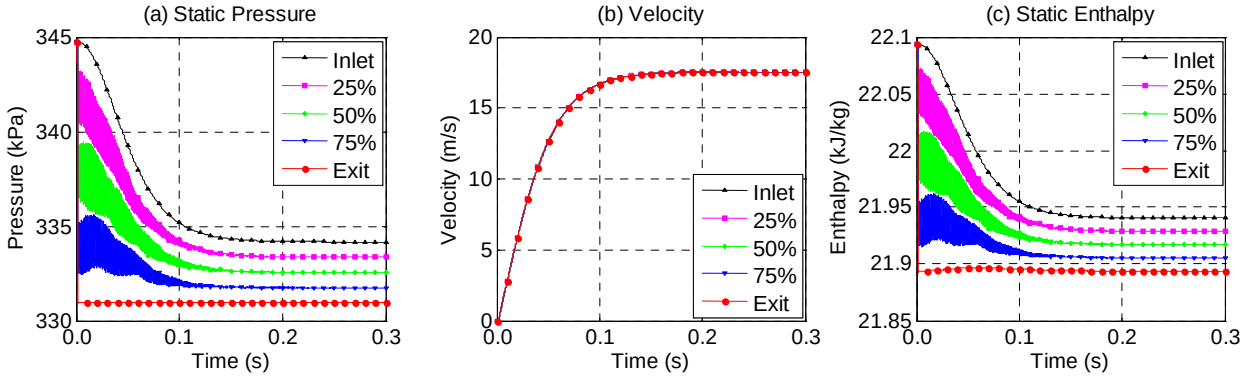

Figure 9. Liquid hydrogen transient pipe flow.

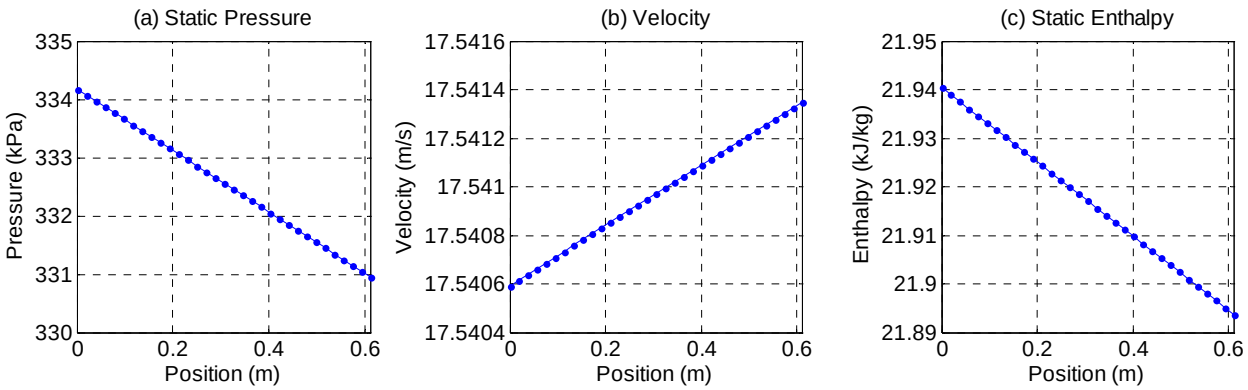

Figure 10. Liquid hydrogen pipe flow at steady-state.

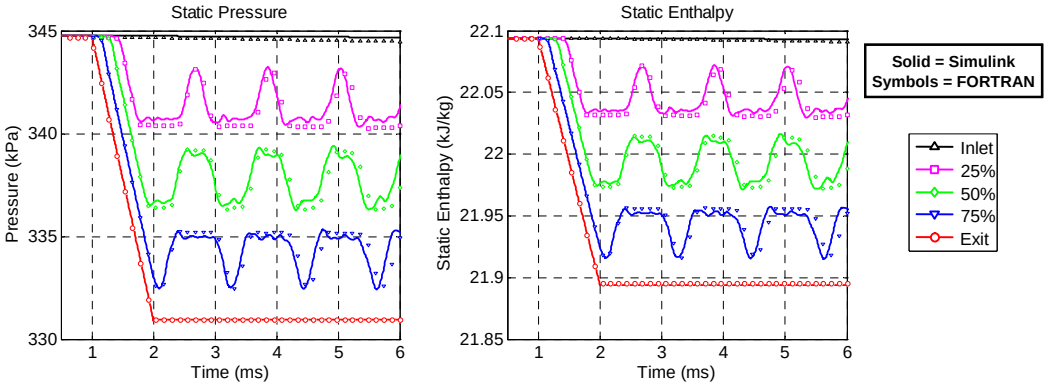

Figure 11. Comparison of hydrogen transient results with Fortran code.

Figures 12 and 13 show the pipe wall temperature history and distribution during the simulation. As shown in Fig. 12, wall temperature decays as flow accelerates and static temperature of the liquid hydrogen is reduced. Wall temperature begins to change first at the pipe outlet since the fluid velocity increases there first. The wall temperature reaches a steady-state distribution within 0.3 seconds. Figure 13 shows the wall temperature distribution along the length of the pipe at several times during the simulation. Initially (t=0), the pipe wall is at a constant temperature. As flow is established at the exit of the pipe, wall temperature drops due to forced convection heat transfer. As flow velocity increases during the simulation, wall temperature continues to drop. At end of the simulation (t=0.3 seconds), the pipe wall has reached a temperature distribution in equilibrium with the fluid static temperature distribution, which is shown as circular symbols in the plot.

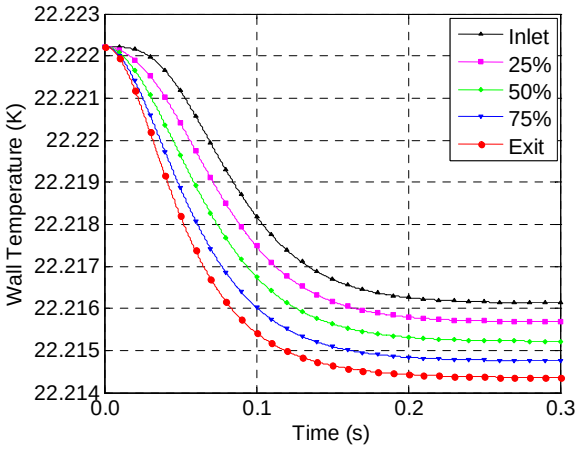

Figure 12. Wall temperature transient.

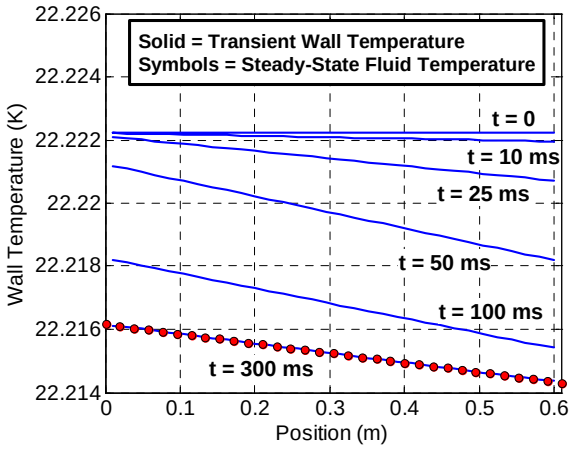

Figure 13. Wall temperature distribution.

As with the previous cases, the steady-state solution can be compared to a hand calculation for the same conditions. The hand calculation yields a flowrate of 0.6109 kg/s (1.3467 lbm/s) and static pressure drop of 3.2222 kPa (0.4673 psid). At steady-state, the simulation indicates a flowrate of 0.6108 kg/s (1.3467 lbm/s) and static pressure drop of 3.2230 kPa (0.4675 psid), or percent differences of 0.004 and 0.02, respectively. The agreement between the incompressible hand calculation and simulation is better for liquid hydrogen compared to gaseous nitrogen, but not as good as water since the compressibility of liquid hydrogen falls between liquid water and gaseous nitrogen.

VI. Conclusion

A new baseline procedure has been developed for the numerical solution of transient quasi-2D flow in lines and volumes including the effects of friction, minor losses, real-fluid properties, and heat transfer between the fluid and bounding wall. The solver is specifically targeted to rocket engine and propulsion system modeling, but can be applied to other types of systems. The procedure has been implemented in both Matlab/Simulink® and Fortran95 using a range of explicit and implicit numerical schemes for the solution of the differential equations to provide flexibility. Real-fluid properties are obtained from a NIST fluid property database, allowing both compressible and incompressible flow problems to be treated using the same procedure. For cases with wall heat transfer, the heat conduction equation is solved simultaneously with the fluid equations to provide conjugate solutions. Various compressible and incompressible unsteady flow test cases are presented to verify solution accuracy against analytical solutions. Future work will focus on extension of the procedure to handle variable flow area, two-phase flow, and acceleration; increasing computational efficiency through the use of parallel computing; and application of the module for system-level analyses.

Acknowledgments

The authors wish to acknowledge the U.S. Air Force Research Laboratory, who funded this program under Contract FA9300-04C-0008, and Mr. Sean Kenny, AFRL program manager for the Upper Stage Engine Technology (USET) program.

References

[1] Wallis, G., *One-Dimensional Two-Phase Flow*, McGraw-Hill, New York, 1969, Chap. 6.
[2] Potter, M.C., Somerton, C.W., *Thermodynamics for Engineers*, Schaum's Outline Series, McGraw-Hill, New York, 1993.
[3] E.B. Wiley, *Fluid Transients in Systems*, Prentice Hall, 1997.
[4] Machmoum, A., Seaïd, M., "A Highly Accurate Modified Method of Characteristics for Convection-Dominated Flow Problems", *Computational Methods in Applied Mathematics*, Vol. 3, No. 4, 2003, pp. 623-646.
[5] Mäkinen, J., Piché, R., Ellman, A., "Fluid Transmission Line Modeling Using a Variational Method", *ASME Journal of Dynamic Systems, Measurement, and Control*, Vol. 122, March 2000, pp. 153-162.
[6] Davis, R.L., Campbell, B.T., "Quasi-2D Unsteady Flow Procedure for Real Fluids," *AIAA 2006-3911*, 2006.
[7] NIST Database 23: NIST REFPROP, Reference Fluid Properties, Software Package, Ver. 7.0, National Institute of Standards and Technology, Boulder, CO.
[8] Anderson, D.A., Tannehill, J.C., Pletcher, R.H., *Computational Fluid Mechanics and Heat Transfer*, Hemisphere, New York, 1984, Chap. 9.
[9] Patankar, S.V., *Numerical Heat Transfer and Fluid Flow*, Hemisphere, New York, 1980, Chap. 4.
[10] Churchill, S.W., "Friction-Factor Equation Spans all Fluid-Flow Regimes", *Chemical Engineering*, Vol. 84, No. 24, November 1977, pp. 91-92.
[11] Pitts, D.R., Sissom, L.E., *Schaum's Outline of Theory and Problems of Heat Transfer*, McGraw-Hill, New York, 1977.
[12] Shampine, L. F. and Reichelt, M. W., "The Matlab ODE Suite", *Society for Industrial and Applied Mathematics Journal on Scientific Computing*, Vol. 18, No. 1, 1997, pp. 1-22.
[13] *Using Simulink*, Version 6.4, The MathWorks, March 2006.
[14] Shampine, L.F. and Hosea, M.E., "Analysis and Implementation of TR-BDF2", *Applied Numerical Mathematics*, v 20, 1996.